A Generalized Analysis for a Class of Rectangular Waveguide Coupler Employing Narrow Wall Slots

A. J. Sangster and Hanyang Wang

Abstract— **A comprehensive analysis is presented which is applicable to the general class of waveguide couplers comprising a dissimilar pair of rectangular waveguide coupled by means of an inclined slot on the narrow wall of the primary waveguide. An entire domain moment method is used to solve a pair of coupled-integral equations for the tangential electric fields on the surfaces of the slot. Three typical examples have been examined to demonstrate the validity of the method. The numerical results are shown to be in good agreement with those obtained from independently procured theoretical evidence and measurements.**

I. Introduction

WAVEGUIDE COUPLERS are fundamental circuit elements in many microwave communication or measurement systems. In the design of the feeding systems for slotted-waveguide antennas, while a variety of waveguide couplers are possible, those based on slot-coupled arrangements are widely used because of their features of high power handling and constructional convenience. A slot-coupled geometry which is of particular interest is one which employs an inclined slot on the narrow wall of rectangular waveguide. Couplers of this class have been introduced into the literature in various forms and treated as separate and distinct aperture discontinuity problems.

The analytical technique for assessing coupling characteristics of the slot-coupled waveguide coupler can be identified as the diffraction theory [1], [2], the variational method [3], [4], the moment method [5], [6] and the hybrid FEM/MoM [7], [8]. A useful contribution on waveguide couplers by means of slots on the narrow wall has recently been presented by Das and Sarma, who have investigated an inclined slot coupled T-junction employing the variational method [9]. However, their method suffers because it is inherently incapable of accommodating the effects of finite wall thickness which is known to have a significant influence on the resonant property of the coupling slot. A moment method formulation has also been applied to the analysis of a narrow wall inclined slot coupler [10]. Here coupling between two dissimilar waveguides is investigated and a parallelogram approximation is introduced to avoid the complicated treatment of inner products involving four components of a dyadic Green's function.

Manuscript received April 10, 1995; revised November 12, 1995. This work was supported by the Engineering and Physics Science Research Council of the United Kingdom.

The authors are with Heriot-Watt University, Department of Computing and Electrical Engineering, Riccarton, Edinburgh, EH14 4AS, UK.

Publisher Item Identifier S 0018-9480(96)01436-6.

In the present paper, a strictly applied moment method analysis is presented for the class of waveguide coupler for which coupling is achieved by means of an inclined slot on the narrow wall of rectangular waveguide. In essence, an equivalence principle is invoked to divide the coupling structure into several separate regions which are then coupled by enforcing the continuity conditions at the interfaces of these regions. The fields in these regions are expressed by appropriate dyadic Green's functions and the surface magnetic currents at the interfaces. This formulation leads to a pair of integral equations in which the magnetic current on the interfaces is unknown. An entire domain moment method is employed to transform the integral equations into a matrix equation using trigonometric basis functions. In contrast to the approach used in [10] which employs a parallelogram approximation to the slot geometry, the inner products are here evaluated strictly to achieve higher accuracy. The resultant matrix equation is then solved using a matrix inversion technique. The theoretical formulation has been validated by three examples. The numerical results are in good agreement with those obtained from independently procured theoretical evidence and measurements.

II. Theory

A. Establishment of the Integral Equations

The general geometry of a class of waveguide couplers by means of an inclined slot on the narrow wall of a rectangular waveguide is illustrated in Fig. 1. The configuration consists of the primary waveguide, the coupling slot, and the coupling region. To satisfy the boundary conditions, the tangential electric field continues over the upper and low surfaces of the slot, namely

$$\overline{n}_1 \times (E_A - E_B) = 0 \qquad \text{on} \quad S_1 \tag{1}$$

$$\overline{n}_2 \times (E_C - E_B) = 0 \qquad \text{on} \quad S_2. \tag{2}$$

where E_Q denotes the electric field in region Q ($Q = A, B, C$) as illustrated in Fig. 2. In accordance with an equivalence principle [11], if the slot is closed by two perfect conductors with two sheets of magnetic current $\overline{M}_1$ and $\overline{M}_2$ on the upper and lower surfaces of the slot, the electromagnetic field remains unchanged. The coupling structure is, therefore, divided into three separate regions, that is, the primary waveguide (region A), the slot cavity (region B) and the coupling

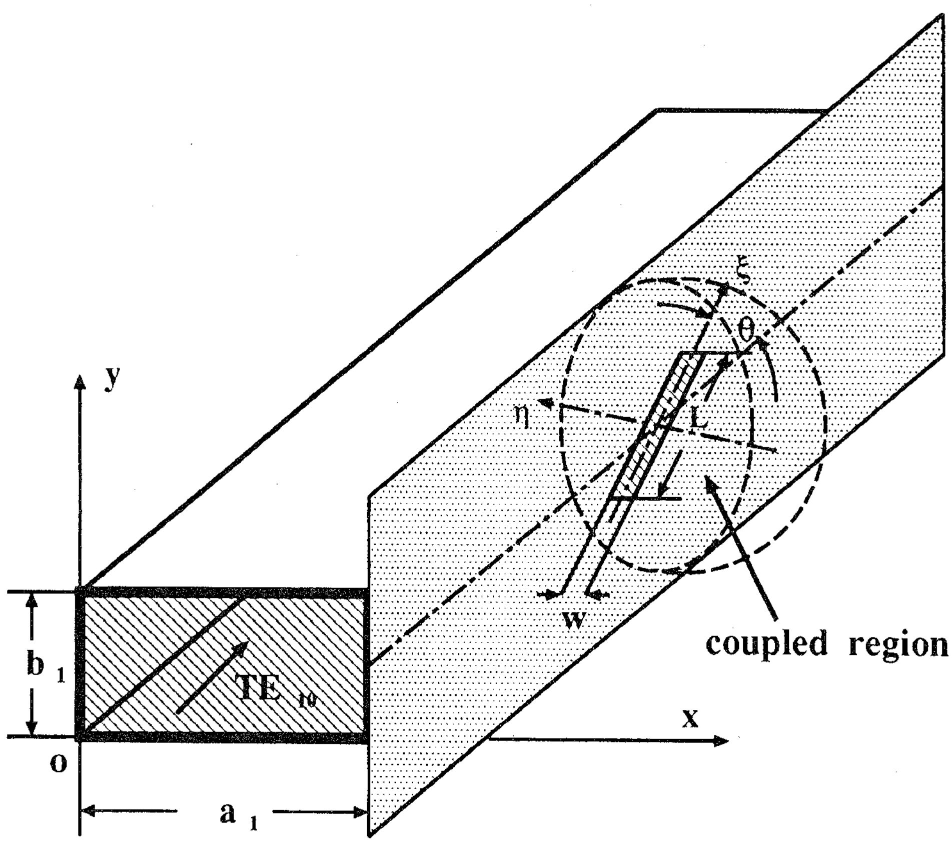

Fig. 1. Geometry of coupling slot on the narrow wall of waveguide.

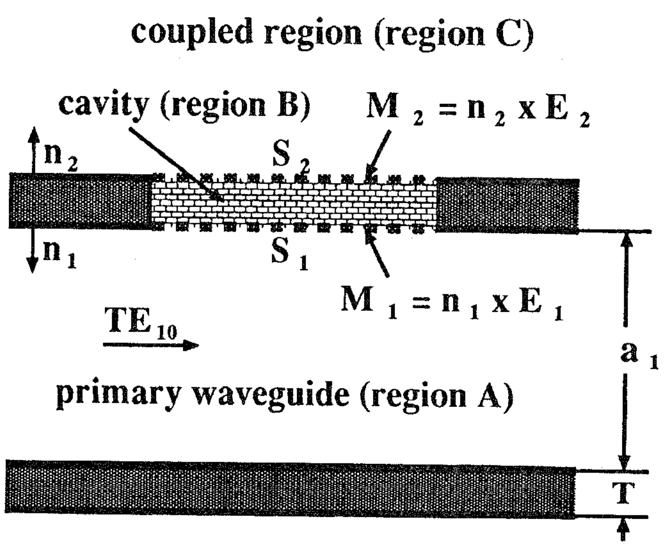

Fig. 2. Division of regions after equivalence.

region (region C). In region A, the electromagnetic field is the sum of the incident field and the field produced by the surface magnetic current $\overline{M}_1$. In region B, the electromagnetic field is the field produced by both surface magnetic currents $\overline{M}_1$ and $\overline{M}_2$. Similarly, the electromagnetic field in region C is the field generated by magnetic current $\overline{M}_2$.

By applying continuity conditions for the tangential component of the magnetic field on the upper and lower surfaces, we obtain

$$\overline{n}_1 \times \overline{H}_B(\overline{r}) - \overline{n}_1 \times \overline{H}_A(\overline{r}) = \overline{n}_1 \times \overline{H}^{in}(\overline{r}) \qquad \text{on } S_1 \quad (3)$$

$$\overline{n}_2 \times \overline{H}_B(\overline{r}) - \overline{n}_2 \times \overline{H}_C(\overline{r}) = 0 \qquad \text{on } S_2 \quad (4)$$

where $\overline{H}_Q$ represents the magnetic field in region Q ($Q = A, B, C$) and $\overline{H}^{in}$ denotes the incident field in region A. If a dyadic Green's function of magnetic type is introduced, which satisfies the following equation

$$\nabla \times \nabla \times \overline{\overline{G}}(\overline{r} \mid \overline{r}_0) - K^2\overline{\overline{G}}(\overline{r} \mid \overline{r}_0) = -\overline{\overline{I}}\delta(\overline{r} - \overline{r}_0) \quad (5)$$

$$\overline{n} \times \nabla \times \overline{\overline{G}}(\overline{r} \mid \overline{r}_0) = 0 \quad (6)$$

with

$$\overline{\overline{I}} = \overline{xx} + \overline{yy} + \overline{zz} \quad (7)$$

it is possible to calculate the magnetic field in each region from

$$\overline{H}(\overline{r}) = j\omega\epsilon \oint \overline{\overline{G}}(\overline{r} \mid \overline{r}_0) \cdot \overline{M}(\overline{r}_0)\, dS_0 \quad (8)$$

where K is the wavenumber, ω is the angular frequency, ϵ is the permittivity, $\overline{\overline{G}}$ is the dyadic Green's function of magnetic type, and $\overline{M}$ is the surface magnetic current. The surface integral is taken over the source region $\overline{r}_0$. If the magnetic fields in the three regions are represented by (8) and the resultant expressions are substituted into (3) and (4), the following integral equations are formed

$$j\omega\epsilon\overline{n}_1 \times \iint_{S_1} [\overline{\overline{G}}_A + \overline{\overline{G}}_B] \cdot \overline{M}_1(\overline{r}_0)\, dS_0 + j\omega\epsilon\overline{n}_1 \times \iint_{S_2} \overline{\overline{G}}_B \cdot \overline{M}_2(\overline{r}_0)\, dS_0 = \overline{n}_1 \times \overline{H}^{in} \quad (9)$$

$$j\omega\epsilon\overline{n}_2 \times \iint_{S_2} [\overline{\overline{G}}_C + \overline{\overline{G}}_B] \cdot \overline{M}_2(\overline{r}_0)\, dS_0 + j\omega\epsilon\overline{n}_2 \times \iint_{S_1} \overline{\overline{G}}_B \cdot \overline{M}_1(\overline{r}_0)\, dS_0 = 0 \quad (10)$$

where $\overline{\overline{G}}_{A,B,C}$ denote the dyadic Green's function in region A, B, and C, respectively.

B. Implementation of the Moment Method

Since it is almost impossible to obtain an analytical solution to the integral equation (9) and (10) due to their complexity, a numerical technique should be used. Because the moment method has provided one of the most accurate means for solving problems of waveguide coupling through slots or apertures, it is employed here to solve the integral equations. As the moment method is well documented in the literature [5], [6], [12], its basic principle is not developed in detail here.

In the search for a moment method solution to the integral equations shown in (9) and (10), the unknown surface magnetic currents are expanded as follows

$$\overline{M}_1(\overline{r}_0) \doteq \overline{n}_1 \times \sum_{s=1}^{N} a_s f_s^1(\overline{r}_0)\overline{\eta} \quad (11)$$

$$\overline{M}_2(\overline{r}_0) \doteq \overline{n}_2 \times \sum_{s=1}^{N} b_s f_s^2(\overline{r}_0)\overline{\eta} \quad (12)$$

where a_s and b_s are the unknown complex expansion coefficients, $f_s^1(\overline{r}_0)$ and $f_s^2(\overline{r}_0)$ are basis functions, s is the order of the basis functions and N is the number of the basis functions. A definition of a set of weighting functions and an inner product are required for the implementation of the moment method. The inner product is chosen, denoted by angular brackets, as

$$\langle\overline{p} \cdot \overline{q}\rangle = \iint_S \overline{p} \cdot \overline{q}\, dS \quad (13)$$

and the weighting functions will be of the same type as the basis functions, namely

$$g_i^1(\overline{r}) = f_i^1(\overline{r}) \quad \text{and} \quad g_i^2(\overline{r}) = f_i^2(\overline{r}) \quad (14)$$

$$i = 1, 2, \cdots, N$$

where i and N are the order and the number of the weighting functions, respectively. Substituting (11) and (12) into (9) and (10) and taking the inner product of the resultant equations with the weighting functions $g_i^1(\overline{r})$ and $g_i^2(\overline{r})$, we obtain a matrix equation

$$\begin{bmatrix} [Y_{is}^{11}] + [Y_{is}^{A}] & [Y_{is}^{12}] \\ [Y_{is}^{21}] & [Y_{is}^{22}] + [Y_{is}^{C}] \end{bmatrix} \begin{bmatrix} [a_s] \\ [b_s] \end{bmatrix} = \begin{bmatrix} [H_i] \\ [Q_i] \end{bmatrix} \quad (15)$$

where

$$Y_{is}^{A} = -j\omega\epsilon \iint_{S_1} g_i^1(\overline{r})\overline{\eta} \cdot \left[\overline{n}_1 \times \iint_{S_1} \overline{\overline{G}}_A(\overline{r} \mid \overline{r}_0) \cdot f_s^1(\overline{r}_0)\overline{\xi}\, dS_0\right] dS \quad (16)$$

$$Y_{is}^{11} = -j\omega\epsilon \iint_{S_1} g_i^1(\overline{r})\overline{\eta} \cdot \left[\overline{n}_1 \times \iint_{S_1} \overline{\overline{G}}_B(\overline{r} \mid \overline{r}_0) \cdot f_s^1(\overline{r}_0)\overline{\xi}\, dS_0\right] dS \quad (17)$$

$$Y_{is}^{12} = +j\omega\epsilon \iint_{S_1} g_i^1(\overline{r})\overline{\eta} \cdot \left[\overline{n}_1 \times \iint_{S_2} \overline{\overline{G}}_B(\overline{r} \mid \overline{r}_0) \cdot f_s^2(\overline{r}_0)\overline{\xi}\, dS_0\right] dS \quad (18)$$

$$Y_{is}^{21} = +j\omega\epsilon \iint_{S_2} g_i^2(\overline{r})\overline{\eta} \cdot \left[\overline{n}_2 \times \iint_{S_1} \overline{\overline{G}}_B(\overline{r} \mid \overline{r}_0) \cdot f_s^1(\overline{r}_0)\overline{\xi}\, dS_0\right] dS \quad (19)$$

$$Y_{is}^{22} = -j\omega\epsilon \iint_{S_2} g_i^2(\overline{r})\overline{\eta} \cdot \left[\overline{n}_2 \times \iint_{S_2} \overline{\overline{G}}_B(\overline{r} \mid \overline{r}_0) \cdot f_s^2(\overline{r}_0)\overline{\xi}\, dS_0\right] dS \quad (20)$$

$$Y_{is}^{C} = -j\omega\epsilon \iint_{S_2} g_i^2(\overline{r})\overline{\eta} \cdot \left[\overline{n}_2 \times \iint_{S_2} \overline{\overline{G}}_C(\overline{r} \mid \overline{r}_0) \cdot f_s^2(\overline{r}_0)\overline{\xi}\, dS_0\right] dS \quad (21)$$

$$H_i = -\iint_{S_1} g_i^1(\overline{r})\overline{\eta} \cdot [\overline{n}_1 \times \overline{H}^{in}(\overline{r})]\, dS \quad (22)$$

$$Q_i = 0. \quad (23)$$

In accordance with earlier observations [5], [13], entire domain sinusoidal basis functions have been preferred, in order to reduce the dimension of the matrix equation and hence to achieve faster convergence. In particular, the basis functions are chosen to be

$$f_s^1(\bar{r}_0) = f_s^2(\bar{r}_0) = \sin\frac{s\pi(\xi_0 + \frac{L}{2})}{L} \tag{24}$$

where ξ_0 is the longitudinal coordinate of the coupling slot and L is slot length.

C. Evaluation of the Matrix Elements

The elements in the matrix equation (15) can be divided into four kinds of elements, namely, the elements associated with the primary waveguide, the slot cavity, the coupling region and the incident field. It should be emphasised here that $m = 0$, $n = 0$ mode should be included in the summation of the waveguide modes. Otherwise, unexpected errors will occur in the vicinity of resonance [14].

Substituting the basis functions and the weighting functions given by (24) and (14) into (16) and performing the vector operation, we can obtain the integral expression for the matrix element in relation to the primary waveguide, namely

$$\begin{aligned} Y_{is}^A = j\omega\epsilon\Big\{ &\sin^2\theta \iint_{S_1} g_i^1(\bar{r}) \cdot \left[\iint_{S_1} G_A^{yy}(\bar{r}\mid\bar{r}_0) f_s^1(\bar{r}_0)\,dS_0\right] dS \\ &+ \sin\theta\cos\theta \iint_{S_1} g_i^1(\bar{r}) \cdot \left[\iint_{S_1} G_A^{yz}(\bar{r}\mid\bar{r}_0) f_s^1(\bar{r}_0)\,dS_0\right] dS \\ &+ \cos\theta\sin\theta \iint_{S_1} g_i^1(\bar{r}) \cdot \left[\iint_{S_1} G_A^{zy}(\bar{r}\mid\bar{r}_0) f_s^1(\bar{r}_0)\,dS_0\right] dS \\ &+ \cos^2\theta \iint_{S_1} g_i^1(\bar{r}) \cdot \left[\iint_{S_1} G_A^{zz}(\bar{r}\mid\bar{r}_0) f_s^1(\bar{r}_0)\,dS_0\right] dS\Big\} \end{aligned} \tag{25}$$

where G_A^{yy}, G_A^{yz}, G_A^{zy} and G_A^{zz} are the components of the waveguide dyadic Green's function given by

$$G_A^{yy}(\bar{r}\mid\bar{r}_0) = \sum_{m=0}^{\infty}\sum_{n=0}^{\infty} A_{mn}\left(1 + \frac{1}{K^2}\frac{\partial^2}{\partial y^2}\right) \cdot [S_x S_{x_0} S_y S_{y_0} \exp(-\Gamma_{mn}|z - z_0|)] \tag{26}$$

$$G_A^{yz}(\bar{r}\mid\bar{r}_0) = \sum_{m=0}^{\infty}\sum_{n=0}^{\infty} A_{mn}\frac{\partial^2}{\partial y\partial z} \cdot [C_x C_{x_0} S_y S_{y_0} \exp(-\Gamma_{mn}|z - z_0|)] \tag{27}$$

$$G_A^{zy}(\bar{r}\mid\bar{r}_0) = \sum_{m=0}^{\infty}\sum_{n=0}^{\infty} A_{mn}\frac{\partial^2}{\partial z\partial y} \cdot [S_x S_{x_0} C_y C_{y_0} \exp(-\Gamma_{mn}|z - z_0|)] \tag{28}$$

$$G_A^{zz}(\bar{r}\mid\bar{r}_0) = \sum_{m=0}^{\infty}\sum_{n=0}^{\infty} A_{mn}\left(1 + \frac{1}{K^2}\frac{\partial^2}{\partial z^2}\right) \cdot [C_x C_{x_0} C_y C_{y_0} \exp(-\Gamma_{mn}|z - z_0|)] \tag{29}$$

where

$$\Gamma_{mn} = \sqrt{K_c^2 - K^2}; \qquad K_c = \sqrt{K_x^2 + K_y^2};$$

$$K_x = \frac{m\pi}{a}; \qquad K_y = \frac{n\pi}{b};$$

$$S_x = \sin(K_x x); \qquad S_{x0} = \sin(K_x x_0);$$

$$S_y = \sin(K_y y); \qquad S_{y0} = \sin(K_y y_0);$$

$$C_x = \cos(K_x x); \qquad C_{x_0} = \cos(K_x x_0);$$

$$C_y = \cos(K_y y); \qquad C_{y_0} = \cos(K_y y_0);$$

$$A_{mn} = \frac{\epsilon_{0m}\epsilon_{0n}}{2ab\Gamma_{mn}}; \qquad \epsilon_{0i} = \begin{cases}1, & \text{if } i = 0;\\ 2, & \text{if } i \neq 0.\end{cases}$$

Substituting the above Green's function into (25) and evaluating the resultant integral, we obtain

$$\begin{aligned} Y_{is}^A = j\omega\epsilon\sum_{m=0}^{\infty}\sum_{n=0}^{\infty} A_{mn1}\Big\{ &-\sin^2\theta\left(1 - \frac{K_{y1}^2}{K^2}\right)\iint_{S_1} g_i^1(\bar{r}) S_{y1} \cdot \left[\iint_{S_1} f_s^1(\bar{r}_0) S_{y_0 1}\exp(-\Gamma_{mn1}|z - z_0|)\,dS_0\right] dS \\ &- \sin\theta\cos\theta\frac{K_{y1}}{K^2}\iint_{S_1} g_i^1(\bar{r}) C_{y1}\frac{\partial}{\partial z} \cdot \left[\iint_{S_1} f_s^1(\bar{r}_0) S_{y_0 1}\exp(-\Gamma_{mn1}|z - z_0|)\,dS_0\right] dS \\ &+ \cos\theta\sin\theta\frac{K_{y1}}{K^2}\iint_{S_1} g_i^1(\bar{r}) S_{y1}\frac{\partial}{\partial z} \cdot \left[\iint_{S_1} f_s^1(\bar{r}_0) C_{y_0 1}\exp(-\Gamma_{mn1}|z - z_0|)\,dS_0\right] dS \\ &- \cos^2\theta\iint_{S_1} g_i^1(\bar{r}) C_{y1}\left(1 + \frac{\partial^2}{K^2\partial z^2}\right) \cdot \left[\iint_{S_1} f_s^1(\bar{r}_0) C_{y_0 1}\exp(-\Gamma_{mn1}|z - z_0|)\,dS_0\right] dS\Big\} \end{aligned} \tag{30}$$

where

$$A_{mn1} = \frac{\epsilon_{0m}\epsilon_{0n}}{2a_1 b_1\Gamma_{mn1}}; \qquad \Gamma_{mn1} = \sqrt{K_{c1}^2 - K^2};$$

$$K_{c1} = \sqrt{K_{x1}^2 + K_{y1}^2}; \qquad K_{x1} = \frac{m\pi}{a_1}; \qquad K_{y1} = \frac{n\pi}{b_1};$$

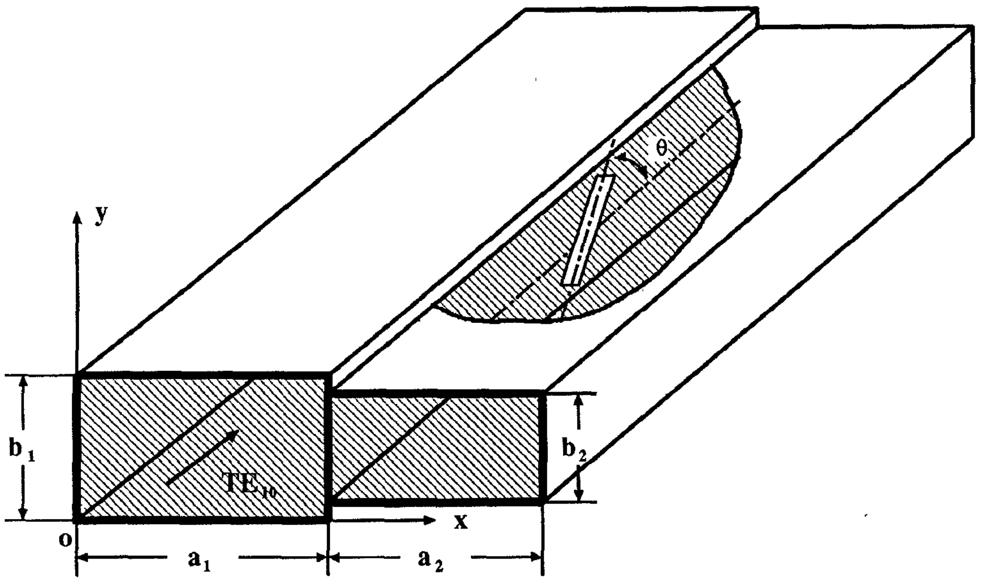

Fig. 3. Slot coupler of dissimilar rectangular waveguides.

$$S_{y1} = \sin(K_{y1}y); \qquad S_{y_01} = \sin(K_{y1}y_0);$$

$$C_{y1} = \cos(K_{y1}y); \qquad C_{y_01} = \cos(K_{y1}y_0).$$

Since the matrix elements associated with the slot cavity have been evaluated previously [5], it is unnecessary to repeat the same procedures here. The evaluation of the elements associated with the coupled region depends on the geometry of the coupled region. Once the exact structure of the slot coupler is determined, the results for the elements can be obtained by following the same procedures used in the evaluation of the matrix element associated with the primary waveguide.

It is assumed that the initial excitation is caused by an incident TE_{10} wave in the primary waveguide. More specifically, the components of this wave are as follows

$$H_x^{in} = H_0 \sin\left(\frac{\pi}{a_1}x\right) \exp(-\Gamma_{101}z) \quad (31)$$

$$E_y^{in} = -Z_{10}H_0 \sin\left(\frac{\pi}{a_1}x\right) \exp(-\Gamma_{101}z) \quad (32)$$

$$H_z^{in} = \frac{\pi}{\Gamma_{101}a_1} H_0 \cos\left(\frac{\pi}{a_1}x\right) \exp(-\Gamma_{101}z) \quad (33)$$

where H_0 denotes the amplitude of the incident wave, Z_{10} is the wave impedance of the dominant mode in the primary waveguide and Γ_{101} is given in (30), that is, let $m = 1$, $n = 0$ in Γ_{mn1}. Substituting the above equations into (22), we obtain

$$H_i = H_0 \cos\theta \frac{\pi}{\Gamma_{101}a_1} \iint_{S_1} g_i^1(\bar{r}) \exp(-\Gamma_{101}z)\, dS. \quad (34)$$

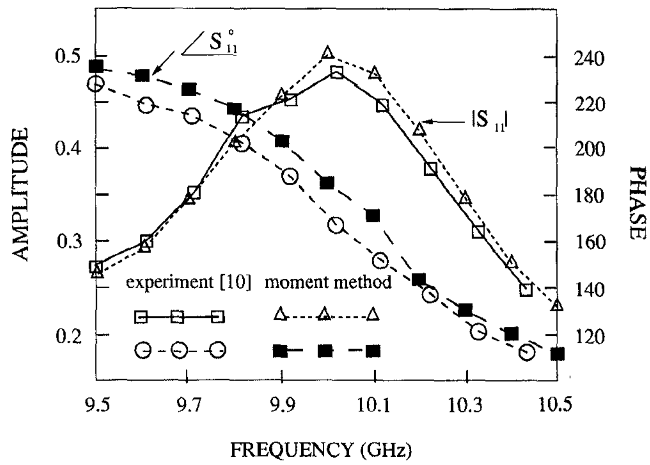

Fig. 4. Reflection coefficient as a function of frequency ($a_1 = a_2 = 22.86$ mm; $b_1 = b_2 = 10.16$ mm; $T = 1.27$ mm; $L = 16.20$ mm; $w = 1.00$ mm; $\theta = 30°$).

D. Expressions for the Scattering Parameters

Despite their length and complexity, the matrix elements can readily be evaluated by means of a computer. As the entire domain sinusoidal basis functions are used, accurate results can be obtained by using only a few terms of the basis functions. Since the dimension of the matrix equation is not large, the matrix equation can be solved by direct matrix inversion to obtain the surface magnetic currents. Once the surface magnetic current is available, the scattering fields in the primary waveguide can be determined by means of (8), namely

$$\bar{H}^{\pm}(\bar{r}) = j\omega\epsilon \sum_{s=1}^{N} \iint_{S_1} \bar{\bar{G}}_a(\bar{r} \mid \bar{r}_0) \cdot \bar{\xi} a_s f_s^1(\bar{r}_0)\, dS_0. \quad (35)$$

Subsequently, the scattering parameters can be evaluated as

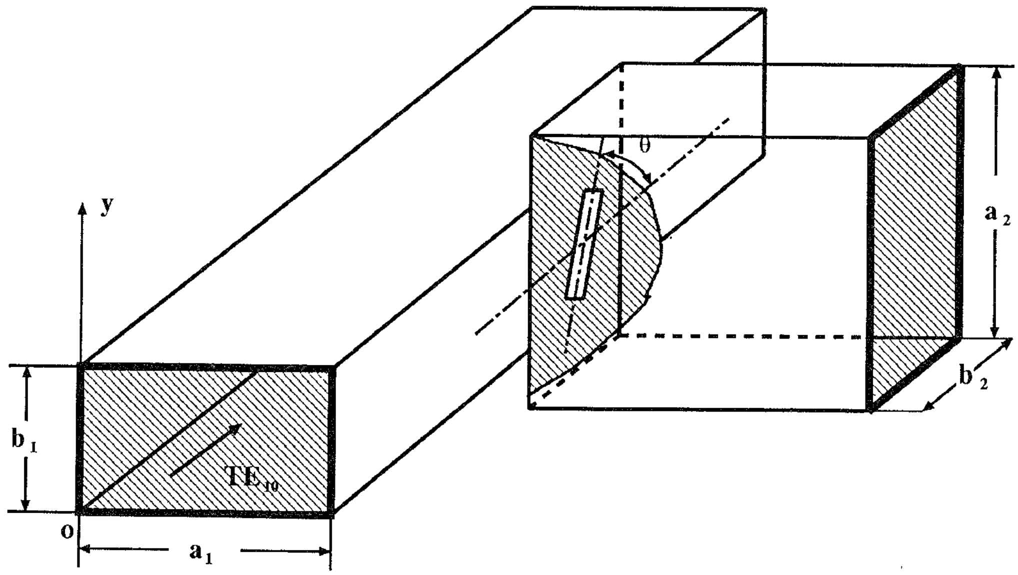

Fig 5. Slot coupled waveguide T-junction (case one).

follows

$$S_{11} = -\frac{H_x^-}{H_x^{in}} = j\omega\epsilon\frac{\pi}{a_1^2 b_1 K^2}\sum_{s=1}^{N} a_s \cdot \iint_{S_1} \cos\theta f_s^1(\bar{r}_0)\exp(-\Gamma_{101}z_0)\,dS_0 \quad (36)$$

$$S_{21} = 1 + \frac{H_x^+}{H_x^{in}} = 1 + j\omega\epsilon\frac{\pi}{a_1^2 b_1 K^2}\sum_{s=1}^{N} a_s \cdot \iint_{S_1} \cos\theta f_s^1(\bar{r}_0)\exp(\Gamma_{101}z_0)\,dS_0. \quad (37)$$

III. Numerical Examples

To validate the moment method formulation presented in the previous section, three coupling geometries are examined, which are commonly used in the design of the feeding systems of slotted-waveguide antennas. In the numerical computations, the convergence of the solutions has been examined, and it is observed that five basis functions are required to achieve a satisfactory accuracy. Consequently, five basis functions are employed throughout in the numerical examples. The CPU time on a HP-9000 work station for the computation of a single numerical point is less than four minutes for all of the examined geometries.

A. Narrow Wall Parallel Coupler

The geometry of the narrow wall coupler reported in [10] is depicted in Fig. 3. To effect a moment method analysis of this problem, a parallelogram approximation to the shape of the inclined slot is employed in the above paper. In the present analysis no such approximation is invoked. Inherently more accurate results are therefore achievable. When the present theory is applied to a 30° inclined slot between similar WG16 waveguides very close agreement with the predictions of [10] is achieved, while good agreement with measurement is demonstrated in Fig. 4, for the magnitude and phase of S_{11} over a range of frequencies in the vicinity of the slot resonance.

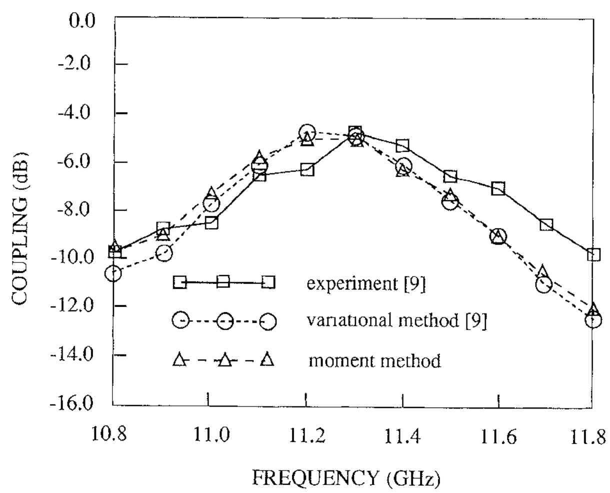

Fig 6. Coupling as a function of frequency ($a_1 = a_2 = 22.86$ mm; $b_1 = b_2 = 10.16$ mm; $T = 1.27$ mm; $L = 14.00$ mm; $w = 0.80$ mm; $\theta = 45°$)

B. Slot Coupled T-Junction (Case 1)

The slot coupled T-junction geometry shown in Fig. 5 has been examined, using a variational analysis, in some detail in [9]. This case can be implemented using the generalized theory of Section II by employing the appropriate components of the Green's function in the secondary guide. In programming terms this is achieved by incorporating optional subroutines which encompass all possible geometrical configurations.

In Fig. 6 the predicted coupling associated with a 45° slot in a T-junction between standard WG16 rectangular waveguides is compared with variational predictions and the measured

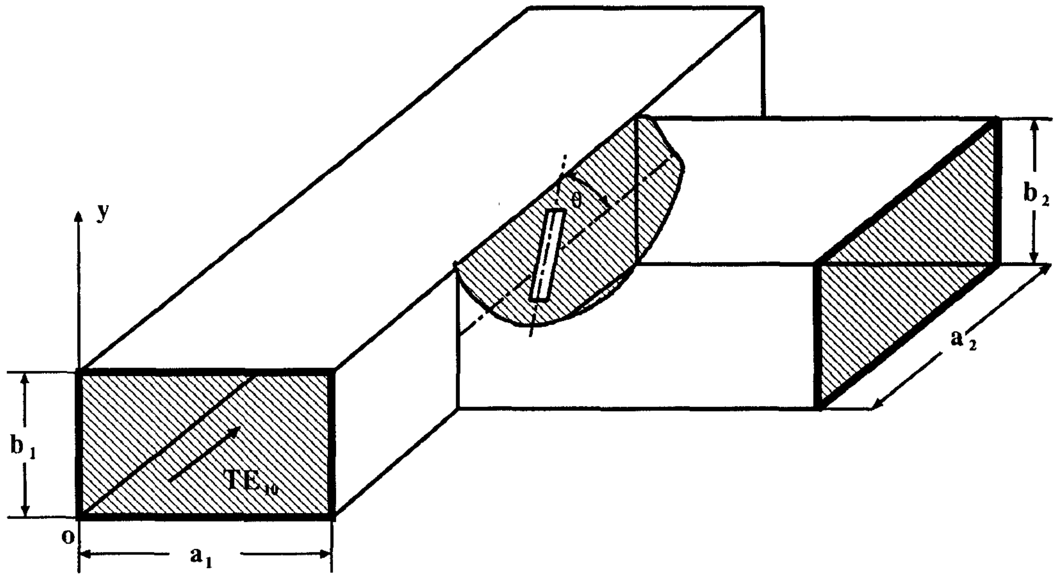

Fig. 7. Slot coupled waveguide T-junction (case two).

results presented in [9]. In the vicinity of resonance close agreement between the theoretical predictions is demonstrated. The deviations between the theoretical curves at frequencies well away from resonance can largely be attributed to the inaccurate treatment of wall thickness effects which is employed in the variational calculations. The agreement with measured results is good when experimental errors are taken into account.

C. Slot Coupled T-Junction (Case 2)

The H-plane T-junction illustrated in Fig. 7 involves simply a 90° rotation of the secondary guide when compared with the geometry of case 1. In mathematical terms this implies that the components of the Green's function for the secondary waveguide should be changed to accommodate to this geometry.

The H-plane Tee coupled by means of a longitudinal slot ($\theta = 0°$) has also been examined, as a separate problem, [15], again using a variational technique. Not unexpectedly, the correlation between the moment method predictions and those of [15], based on this author's variational approach, follows the pattern discussed above. Agreement between our theory and experiment for a coupling slot with 0° inclination in a WG16 H-plane Tee is good, as Fig. 8 illustrates. Theoretical predictions for the coupling provided by slots with inclinations which are greater than 0° are also shown for comparison. The inclined slot case is not accommodated in the analysis of [15].

IV. Conclusion

An analysis, based on the moment method, has been developed which is capable of treating a general class of rectangular waveguide coupling problem where slot coupling through the side wall of the primary guide is involved. The method has been applied to three coupler geometries which have previously been treated in the literature as separate problems. In all the three cases, good agreement between the proposed generalized theory and other analytical techniques is demonstrated. The results are also supported by measurements.

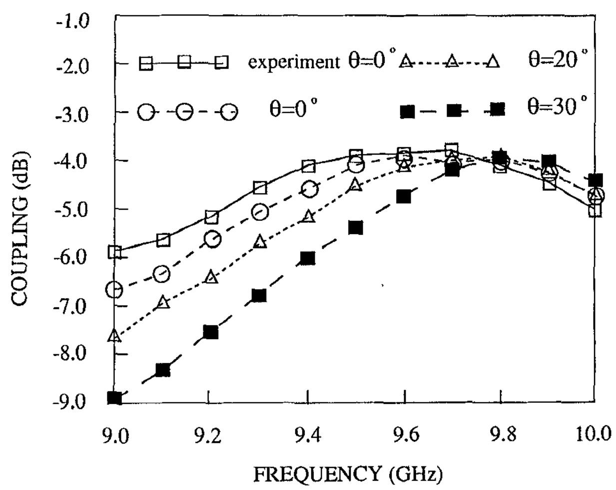

Fig. 8. Coupling as a function of frequency ($a_1 = a_2 = 22.86$ mm; $b_1 = b_2 = 10.16$ mm; $T = 1.27$ mm; $L = 16.00$ mm; $w = 0.80$ mm).

References

[1] H. A. Bethe, "Theory of diffraction by small holes," *Phys. Rev*, vol. 66, pp. 163–182, 1944.
[2] S. B. Cohn, "Electric polarizability of apertures of arbitrary shape," *Proc. IRE*, vol. 40, pp. 1069–1071, 1952.
[3] A. A. Oliner, "The impedance properties of narrow radiating slots in the broad face of rectangular waveguide, Part I-Theory," *IRE Trans. Antennas Propagat.*, vol. AP-5, pp. 4–20, 1957.
[4] A. J. Sangster, "Slot coupling between uniform rectangular waveguides," *IEEE Trans. Microwave Theory Tech.*, vol. MTT-27, pp. 705–707, 1979.
[5] R. W. Lyon and A. J. Sangster, "Efficient moment method analysis of radiating slots in a thick-walled waveguide," *Proc. Inst. Elec. Eng.*, vol. 128, pt. H, pp. 197–205, 1981.
[6] G. T. Stern and R. S. Elliott, "Resonant length of longitudinal slots and validity of circuit representation: theory and experiment," *IEEE Trans. Antennas Propagat.*, vol. AP-33, pp. 1264–1271, 1985.

[7] A. J. Sangster and H. Wang, "Hybrid analytical technique for waveguide coupling by means of aperture or slot," *Microwave Opt. Technol. Lett.*, vol. 6, pp. 829–831, 1993.
[8] J. M. Jin and S. W. Lee, "Hybrid finite-element analysis of scattering and radiation by a class waveguide-fed structures," *Microwave Opt. Technol. Lett.*, vol. 7, pp. 798–803, 1994.
[9] B. N. Das and N. V. S. Sarma, "Analysis of E-H plane Tee junction using a variational formulation," *IEEE Trans. Microwave Theory Tech.*, vol. 39, pp. 1770–1773, 1991.
[10] D. Satyanarayana and A. Chakraborty, "Analysis of wide inclined slot coupled narrow wall coupler between dissimilar rectangular waveguides," *IEEE Trans. Microwave Theory Tech.*, vol. 42, pp. 914–917, 1994.
[11] R. F. Harrington, *Time-harmonic electromagnetic fields.* New York: McGraw-Hill, 1961.
[12] ——, *Field computation by moment methods.* New York: Macmillan, 1968.
[13] A. J. Sangster and H. Wang, "Moment method analysis of a horizontally polarised omnidirectional slot array antenna," *Proc. Inst. Elec. Eng.*, vol. 142, pt. H, pp. 1–6, 1995.
[14] A. J. Sangster and A. H. I. McCormick, "Some observation on the computer-aided design/synthesis of slotted-waveguide antennas," *Int. J. Electronics,* vol. 62, pp. 641–662, 1987.
[15] B. N. Das, N. V. S. Sarma, and A. Chakraborty, "A rigorous variational formulation of an H plane slot-coupled Tee junction," *IEEE Trans. Microwave Theory Tech.*, vol. 38, pp. 93–95, 1990.

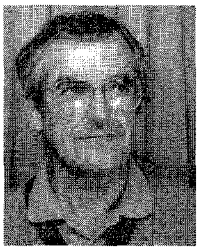

A. J. Sangster received the B.Sc. degree in 1963, the M.Sc. degree in 1964, and the Ph.D. degree in 1967, all from the University of Aberdeen in Scotland.

He spent four years with Ferranti plc. Edinburgh, doing research in wide-band traveling wave tubes, and three years with Plessey Radar plc. U.K., investigating and developing microwave devices and antennas for microwave landing systems and frequency scanned radar systems. Since 1972, he has been with the Heriot-Watt University, Edinburgh, where he became a Professor of Electromagnetic Engineering in 1989. His current research interests lie in the areas of microwave antennas, electrostatically driven micromotors, microwave and mm-wave electron beam tubes, and the numerical solution of electromagnetic radiation and scattering problems. He is the author of over 80 scientific papers on these topics.

Dr. Sangster is a Fellow of the Institution of Electrical Engineers (UK), and a Member of the Electromagnetics Academy (USA).

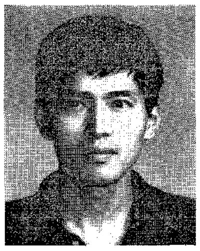

Hanyang Wang received the M.Eng. degree in 1986 from the Northwestern Polytechnic University, China, and the Ph.D. degree in 1994 from the Heriot-Watt University, Edinburgh, U.K.

From 1986 to 1991, he was employed at the Department of Electrical Engineering of the Shandong University, Jinan, China, where he served as an Assistant Lecture, Lecturer, and Associated Professor. From 1994 to 1995, he was a Research Associate in the Heriot-Watt University, Edinburgh. Currently, he is a Senior Research Officer in the Department of Electronic System Engineering of the University of Essex, U.K. His research interests include microwave devices, antennas and antenna arrays, and numerical methods for the solution of electromagnetic radiation and scattering problems.